Inorganic Chemistry

Article

pubs.acs.org/IC

Exploration of Chemically Cross-Linked Metal−Organic Frameworks

C. A. Allen and S. M. Cohen*

Department of Chemistry and Biochemistry, University of California, San Diego, 9500 Gilman Dr. La Jolla, San Diego, California 92093-0358, United States

Supporting Information

ABSTRACT: A series of geometrically constrained, cross-linked benzene dicarboxylic acid (bdc) derivatives have been synthesized and incorporated into the canonical isoreticular metal−organic framework (IRMOF) lattice. Only certain cross-links, which allow for the proper relative orientation of the bdc subunits, form the desired IRMOF. Design criteria from these cross-linked ligands allowed for the rational design of two oligomeric ligands composed of three bdc monomers tethered together. These oligomeric ligands were also readily incorporated into an IRMOF lattice with a high degree of crystallinity and porosity, providing a new dimension to rational ligand design for metal−organic frameworks.

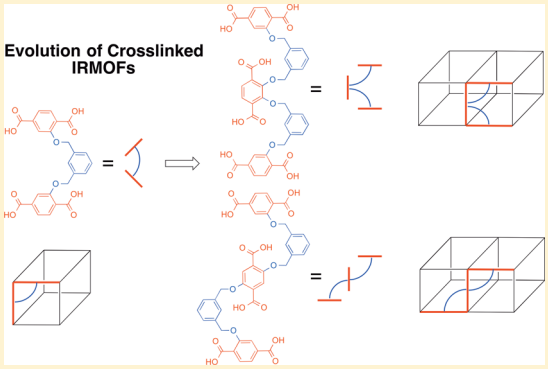

INTRODUCTION

Since the discovery of metal−organic frameworks (MOFs)[1] many efforts have been made to optimize our ability to design and control all facets of these materials including creating more complex architectures.[2,3] MOFs (sometimes referred to as porous coordination polymers, PCPs) are known for being versatile platforms for designing materials that arrange in predicted periodic structures upon crystallization. The tunability of these hybrid materials has been a large factor in their proposed adaptation for a multitude of applications.[4,5] For any given application, the desired characteristics of a material can be engineered by careful choice of the initial building blocks[6] and then fine-tuned with other synthetic methods, such as postsynthetic modification (PSM).[7−12] In a particularly striking example by Sada and co-workers,[13] a crystalline MOF was transformed into a polymer gel by PSM cross-linking, followed by removal of the metal component. The level of chemical cross-linking achieved was sufficient that upon removal of the structural metal ions from the secondary building units (SBUs), the overall morphology of the crystal was preserved in the polymer gel monolith. This spectacular study bridges "hard" crystalline materials with "soft" polymeric materials allowing for the creation of a new area of materials research that harbors characteristics of both classes of compounds.[14−16]

Recently, we described an alternative, presynthetic approach to cross-linked MOFs. IRMOFs were prepared from cross-linked ligands,[17] derived from 2-amino-1,4-benzenedicarboxylic acid (NH_2-bdc). These cross-linked ligands were synthesized by tethering two bdc monomer building blocks with an alkane linker. By direct solvothermal synthesis, these ligands could generate isoreticular metal−organic framework (IRMOF) analogues. Experimental and computational data concluded that the NH_2-bdc tethers were structurally incorporated into the framework, but the flexibility of the linkers resulted in a random orientation of the cross-linking alkyl groups. It was proposed that at least four distinct cross-link orientations were possible for some of these alkyl bridges (Figure S1, Supporting Information).[17] Herein we report a substantial extension of these cross-linked building blocks. The ligands reported herein are geometrically preorganized to reliably form the prototypical IRMOF-1 lattice (Figure 1) with a single linker orientation. More importantly, these cross-linked ligands allowed for the rational design of oligomeric ligands that also produced the canonical IRMOF-1 structure. These studies provide a complementary, bottom-up approach that may lead to the synthesis of polymer-MOF hybrid materials.

EXPERIMENTAL SECTION

General. Starting materials and solvents were purchased and used without further purification from commercial suppliers (Sigma-Aldrich, Alfa Aesar, EMD, TCI, Cambridge Isotope Laboratories, Inc., and others). Chromatography was performed using a CombiFlash Rf 200 automated system from TeledyneISCO (Lincoln, USA). ^{1}H NMR spectra were collected on a Varian Mercury spectrometer running at 400 MHz. Mass spectrometry (MS) was performed at the Molecular Mass Spectrometry Facility (MMSF) in the Department of Chemistry & Biochemistry at the University of California, San Diego. Dimethyl 2-hydroxyterephthalate (**1**, Scheme 1) and dimethyl 2,3-dihydroxyterephthalate (**7**) were synthesized according to literature procedures.[18]

Compound **2**. Compound **1** (1.6 g, 7.7 mmol) was dissolved in *N*,*N*-dimethylformamide (DMF) (15 mL). 1,5-Dibromopentane (0.5 mL, 3.67 mmol) and K_2CO_3 (2.0 g, 14.7 mmol) were added to the solution, and the mixture was stirred at 80 °C overnight. After the mixture was cooled to room temperature, the K_2CO_3 was removed by filtration, and excess water was added to precipitate out a beige solid

Received: April 25, 2014
Published: June 19, 2014

   dx.doi.org/10.1021/ic500951b | *Inorg. Chem.* 2014, 53, 7014−7019

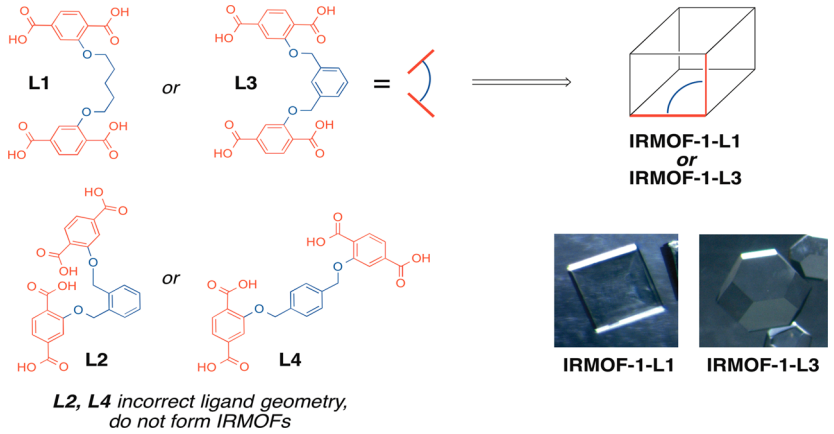

Figure 1. Schematic representation of cross-linked ligands and resulting IRMOFs (photographs shown). IRMOFs were only formed with **L1** and **L3**, where the bdc units can arrange in a specific relative orientation with respect to one another.

that was isolated by vacuum filtration. Yield: 1.0 g (59%). ^{1}H NMR (400 MHz, $CDCl_3$, 35 °C): δ 1.73 (m, 2H; CH_2), 1.95 (m, 4H, CH_2), 3.89 (s, 6H, CO_2CH_3), 3.93 (s, 6H, CO_2CH_3), 4.13 (t, 4H; CH_2), 7.60 (d, 4H; ArH), 7.8 (d, 2H; ArH). ESI-MS(+): m/z 489.23 $[M + H]^+$, 506.22 $[M + NH_4]^+$, 511.19 $[M + Na]^+$.

*Compound **L1**.* Compound **2** (0.7 g, 1.4 mmol) was dissolved in 1:1 v:v THF/4% $KOH_{(aq)}$ solution (30 mL) and stirred overnight at room temperature. The aqueous layer was collected and acidified to pH ≈ 1 with 1 M HCl. A white precipitate formed that was collected by vacuum filtration. Yield (0.61 g, ~99%). ^{1}H NMR (400 MHz, DMSO-d_6, 35 °C): δ 1.61 (m, 2H; CH_2), 1.77 (m, 4H, CH_2), 4.08 (t, 4H; CH_2), 7.52 (m, 4H; ArH), 7.65 (d, 2H; ArH). ESI-MS(−): m/z 431.40$[M - H]^-$.

General Synthesis for Compounds L2–L4. Compound **1** (2.0 g, 9.5 mmol) was dissolved in DMF (100 mL). The appropriate bis(bromomethyl)benzene isomer (1,2-; 1,3-; or 1,4-; 1.2 g, 4.5 mmol) and K_2CO_3 (2.5 g, 18 mmol) were added, and the mixture was stirred at 80 °C overnight. After the mixture was cooled to room temperature, the K_2CO_3 was removed by filtration. Excess water was added to precipitate out a white solid that was isolated by vacuum filtration and washed with minimal acetone. The resulting intermediate (compounds **3**, **4**, or **5**) was dissolved in 1:1 v:v THF/4% KOH(aq) solution (30 mL) and stirred overnight at room temperature. The aqueous layer was collected and acidified to pH ≈ 1 with 1 M HCl. A white precipitate formed that was collected by vacuum filtration. Characterization for compounds **4** and **L3** is given below; similar data for **L2** and **L4** and their associated intermediates can be found in the Supporting Information.

*Compound **4**.* Yield: 1.65 g (70%). ^{1}H NMR (400 MHz, $CDCl_3$, 35 °C): δ 3.92 (d, 12H; CO_2CH_3), 5.25 (s, 4H, CH_2), 7.47 (m, 3H, ArH), 7.60 (s, 1H; ArH), 7.66 (s, 2H; ArH), 7.68 (s, 2H; ArH), 7.85 (d, 2H; ArH). ESI-MS(+): m/z 540.12 $[M + NH_4]^+$, 545.23 $[M + Na]^+$.

*Compound **L3**.* Yield: 1.0 g (~99%). ^{1}H NMR (400 MHz, DMSO-d_6, 35 °C): δ 5.26 (s, 4H; CH_2), 7.43 (m, 1H; ArH), 7.48 (m, 2H; ArH), 7.57 (d, 2H; ArH), 7.59 (s, 1H; ArH), 7.70 (m, 4H; ArH). ESI-MS(−): m/z 465.37 $[M - H]^-$.

*Compound **6**.* Compound **1** (2.9 g, 13.8 mmol) was dissolved in MeCN (150 mL). 1,3-Bis(bromomethyl)benzene (7.3 g, 27.7 mmol) and K_2CO_3 (2.3 g, 16.6 mmol) were added, and the mixture was stirred at 40 °C overnight. After being cooled to room temperature, the K_2CO_3 was removed by filtration, and the solvent removed under a vacuum to reveal a beige solid. A SiO_2 column using 5% ethyl acetate (EtOac) in hexanes as eluent was used to remove excess dibromide, and the eluent was changed to 100% CH_2Cl_2 to liberate the product as a white solid upon removal of solvent. Yield: 4.0 g (74%). ^{1}H NMR (400 MHz, $CDCl_3$, 35 °C): δ 3.94 (s, 6H; CO_2CH_3), 4.52 (s, 2H, CH_2), 5.22 (s, 2H, CH_2), 7.36 (m, 2H; ArH), 7.43 (d, 1H; ArH), 7.56 (s, 1H; ArH), 7.66 (m, 2H; ArH), 7.86 (d, 1H; ArH). ESI-MS(+): m/z 392.79 $[M + H]^+$, 409.70 $[M + NH_4]^+$.

*Compound **8**.* Compound **7** (0.52 g, 2.3 mmol)[18] was dissolved in DMF (100 mL). Compound **6** (2.0 g, 5.1 mmol) and K_2CO_3 (1.3 g, 9.3 mmol) were added, and the mixture was stirred at 80 °C overnight. After being cooled to room temperature, the K_2CO_3 was filtered off, and the solvent removed under a vacuum to yield a beige solid. The product was purified by trituration with acetone followed by vacuum filtration to give a white solid. Yield: 1.0 g (44%). ^{1}H NMR (400 MHz, $CDCl_3$, 35 °C): δ 3.88 (t, 16H; CO_2CH_3), 5.09 (s, 4H, CH_2), 5.14 (s, 4H, CH_2), 7.36 (s, 4H; ArH), 7.48 (s, 4H; ArH), 7.58 (s, 2H; ArH), 7.62 (s, 4H; ArH), 7.80 (d, 2H; ArH). ESI-MS(+): m/z 873.17 $[M + NH4]^+$, 874.18 $[M + Na]^+$, 889.10 $[M + K]^+$.

*Compound **L5**.* Compound **8** was dissolved in 1:1 (v:v) THF/4% KOH(aq) solution (30 mL) and stirred overnight at room temperature. The aqueous layer was collected and acidified to pH ≈ 1 with 1 M HCl. A white precipitate formed that was collected by vacuum filtration. Yield: 0.4 g (65%). ^{1}H NMR (400 MHz, DMSO-d_6, 35 °C): δ 5.05 (s, 4H; CH_2), 5.12 (s, 4H, CH_2), 7.33 (s, 4H; ArH), 7.43 (d, 2H; ArH), 7.48 (t, 4H; ArH), 7.50 (d, 2H; ArH), 7.62 (s, 2H; ArH), 7.68 (d, 2H; ArH). ESI-MS(−): m/z 765.21 $[M - H]^-$, 787.10 $[M + Na\text{-}2H]^-$, 803.11 $[M + K\text{-}2H]^-$, 809.10 $[M + 2Na\text{-}3H]^-$.

*Compound **9**.* Diethyl-2,5-dihydroxyterephthalate (0.44 g, 1.7 mmol) was dissolved in DMF (100 mL). Compound **6** (1.5 g, 3.8 mmol) and K_2CO_3 (0.96 g, 6.9 mmol) were added, and the mixture was stirred at 80 °C overnight. After the mixture was cooled to room temperature, the K_2CO_3 was filtered off, and the solvent removed under a vacuum to reveal a beige solid. The product was purified by trituration with acetone followed by vacuum filtration to give a white solid. Yield: 1.1 g (64%). ^{1}H NMR (400 MHz, $CDCl_3$, 35 °C): δ 1.31 (t, 6H; CH_2CH_3), 3.9 (d, 12H; CO_2CH_3), 4.34 (q, 4H; CH_2CH_3), 5.16 (s, 4H, CH_2), 5.24 (s, 4H, CH_2), 7.43 (m, 2H; ArH), 7.49 (s, 6H; ArH), 7.58 (s, 2H; ArH), 7.70 (d, 2H; ArH), 7.83 (s, 2H; ArH), 7.85 (d, 2H; ArH). ESI-MS(+): m/z 901.22 $[M + Na]^+$.

*Compound **L6**.* Compound **9** was dissolved in 1:1 (v:v) THF/4% KOH(aq) solution (30 mL) and stirred overnight at room temperature. The aqueous layer was collected and acidified to pH ≈ 1 with 1 M HCl. A white precipitate formed that was collected by vacuum filtration. Yield: 1.6 g (86%). ^{1}H NMR (400 MHz, DMSO-d_6, 35 °C): δ 5.15 (s, 4H; CH_2), 5.24 (s, 4H, CH_2), 7.44 (m, 8H; ArH), 7.56 (m, 4H; ArH), 7.69 (m, 4H; ArH). ESI-MS(−): m/z 765.16 $[M - H]^-$, 787.09 $[M + Na\text{-}2H]^-$, 803.09 $[M + K\text{-}2H]^-$, 809.17 $[M + 2Na\text{-}3H]^-$.

*Preparation of IRMOF-1-**L1**, IRMOF-1-**L3**.* $Zn(NO_3)_2{\cdot}6H_2O$ (0.342 g, 1.15 mmol) and a cross-linked ligand (**L1**, **L3**, 0.2 mmol) were dissolved in DMF (5 mL) in a scintillation vial (20 mL). The vial was placed in a sand bath that was placed in a programmable oven. The temperature was raised from room temperature to 100 °C at 2.5 °C/min, held for 24 h, and cooled at 2.5 °C/min to room temperature. Clear blocks (**L1**) or truncated cubes (**L3**) were formed (Figure 1). Once the vial cooled to room temperature, the mother liquor was decanted, and the crystals were washed with DMF (3 × 10 mL), rinsed

dx.doi.org/10.1021/ic500951b | Inorg. Chem. 2014, 53, 7014−7019

Scheme 1. Synthetic Scheme for Selected Compounds[a]

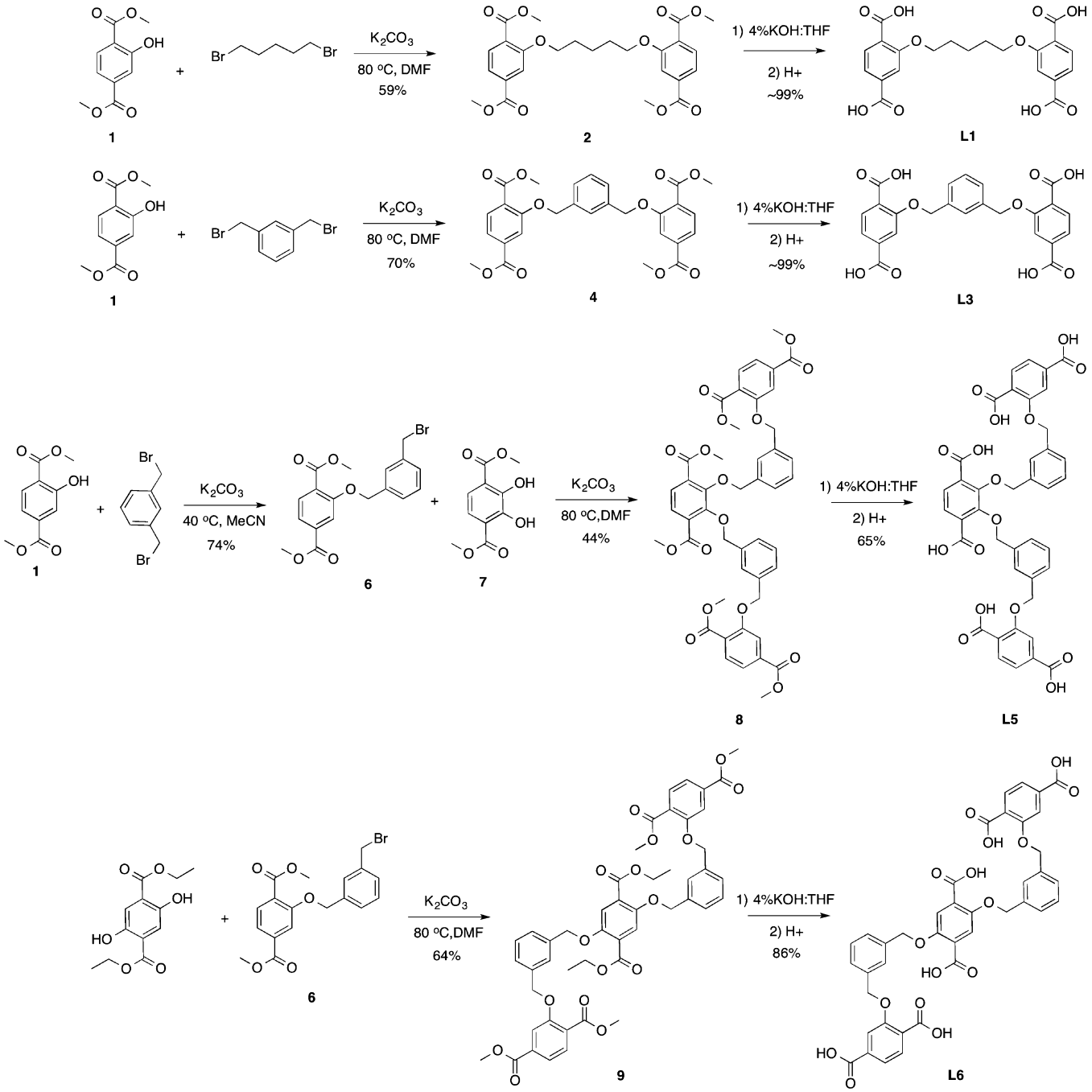

[a]Williamson ether chemistry is utilized to crosslink the bdc subunits, followed by hydrolysis to obtain ligands **L1**, **L3**, **L5**, and **L6**.

with $CHCl_3$ (2 × 10 mL), and left to soak for 3 days with fresh $CHCl_3$ added every 24 h. The crystals were stored in $CHCl_3$ until needed. Yield: IRMOF-1-**L1** 186 mg (>100% due to trapped solvent, FW 920.04 g/mol for $Zn_4OL1_{1.5}$). IRMOF-1-**L3** 147 mg (76%, FW 971.07 g/mol for $Zn_4OL3_{1.5}$). Under the same reaction conditions, **L2** gave no crystals or precipitate, and **L4** gave only an amorphous powder. A variety of other solvothermal conditions were also explored with **L2** and **L4** (Table S1, Supporting Information), but no crystalline products were obtained.

*Preparation of IRMOF-1-**L5**.* $Zn(NO_3)_2{\cdot}6H_2O$ (0.29 g, 0.97 mmol) and **L5** (0.063 g, 0.08 mmol) were dissolved in DMF (5 mL) in a scintillation vial (20 mL). The vial was placed in a sand bath that was placed in a programmable oven. The temperature was raised from room temperature to 100 °C at 0.5 °C/min, held for 24 h and cooled at 0.5 °C/min to room temperature. The product formed as transparent yellow blocks. Yield: 22 mg (22%, FW 1038.13 g/mol for Zn_4OL5).

*Preparation of IRMOF-1-**L6**.* $Zn(NO_3)_2{\cdot}6H_2O$ (0.257 g, 0.86 mmol) and **L6** (0.063 g, 0.08 mmol) were dissolved in 5 mL of DMF in a scintillation vial (20 mL). The vial was placed in a sand bath that was placed in a programmable oven. The temperature was raised from room temperature to 100 °C at 0.5 °C/min, held for 24 h, and cooled at 0.5 °C/min to room temperature. The product formed as clear blocks. Yield: 55 mg (53%, FW 1038.13 g/mol for Zn_4OL6).

Digestion and Analysis by ^1H NMR. ^1H NMR spectra were recorded on a Varian FT-NMR spectrometer (400 MHz). Approximately 5 mg of IRMOF was immediately used after BET analysis and digested with sonication in 500 μL of DMSO-d_6 and 100

dx.doi.org/10.1021/ic500951b | Inorg. Chem. 2014, 53, 7014−7019

μL of dilute DCl (23 μL of 35% DCl in D_2O diluted with 1.0 mL of DMSO-d_6) prior to ^{1}H NMR analysis.

Digestion and Analysis by ESI-MS. ESI-MS was performed using a ThermoFinnigan LCQ-DECA mass spectrometer, and the data were analyzed using the Xcalibur software suite. Samples for ESI-MS analysis were prepared by diluting 10 μL of digested ^{1}H NMR solution in 1 mL of MeOH.

Thermal Analysis. Approximately 10−15 mg of IRMOF (dried after gas sorption analysis) was used for TGA measurements. Samples were analyzed under a stream of dinitrogen (10 mL/min) using a TA Instrument Q600 SDT running from room temperature to 600 °C with a scan rate of 5 °C/min.

PXRD Analysis. Approximately 15 mg of IRMOF (soaked in DMF) was air-dried (~10 min) before PXRD analysis. Powder X-ray diffraction (PXRD) data were collected at ambient temperature on a Bruker D8 Advance diffractometer using a LynxEye detector at 40 kV, 40 mA for Cu Kα (λ = 1.5418 Å), with a scan speed of 1 s/step, a step size of 0.02 in 2θ, and a 2θ range of 5−40°.

BET Surface Area Analysis. Approximately 35−60 mg of IRMOF (previously soaking in $CHCl_3$) was evacuated on a vacuum line for ~1 min at room temperature. The sample was then transferred to a preweighed sample tube and degassed at 105−150 °C on an Micromeritics ASAP 2020 Adsorption analyzer for a minimum of 12 h or until the outgas rate was <5 μmHg. The sample tube was reweighed to obtain a consistent mass for the degassed sample. BET surface area (m^2/g) measurements were collected on three independent samples, unless residual solvent was still present, of each MOF at 77 K with dinitrogen on an Micromeritics ASAP 2020 Adsorption analyzer using the volumetric technique.

RESULTS AND DISCUSSION

The first target of this study was an alkyl linked HO-bdc (**L1**), which was similar to our previously reported systems,[17] but utilizes an ether, rather than an amide linker. This target ligand is an analogue to the shortest tether previously described[17] and was designed to confirm that small changes in the chemical composition of the cross-link (i.e., ether vs amide) would be tolerated during IRMOF formation. Using the well-established Williamson ether synthesis, gram quantities of ligand **L1** were readily obtained (Scheme 1).[19] Consistent with our earlier findings, **L1** produces the desired cross-linked IRMOF as transparent blocks (IRMOF-1-**L1**) under standard solvothermal procedures for an IRMOF material.[20] Extrapolation from a prior computational analysis suggested that this short tether must force the bdc monomers into an adjacent, orthogonal conformation (isomer 1, Figure S1, Supporting Information) based on length and geometric requirements. Powder X-ray diffraction (PXRD) of IRMOF-1-**L1** matches that of IRMOF-1 (Figure 2), and the connectivity and topology was unambiguously confirmed by single-crystal X-ray diffraction (XRD, Table S2). As expected, the alkyl linker was disordered and could not be located but was determined to be present and intact by ^{1}H NMR and mass spectral analysis of acid digested IRMOF-1-**L1** (Figure S2). After extensive rinsing with $CHCl_3$ and heating to 150 °C under a vacuum, significant amounts of DMF remained trapped in IRMOF-1-**L1**, similar to that observed with other cross-linked MOFs.[17] Thermogravimetric analysis (TGA) shows a ~5% weight loss at just under 200 °C, indicative of trapped solvent (Figure 3), followed by decomposition of the framework at ~380 °C, which is typical for IRMOFs. Activated IRMOF-1-**L1** gave a Brunauer−Emmett−Teller (BET) surface areas of 1711 m^2/g and 1450 m^2/g when activated at 150 and 105 °C, respectfully, consistent with greater solvent trapping at lower temperature. In contrast, typical, unlinked IRMOFs will release all solvent guests under the aforementioned activation conditions.[21] The trapped solvent in this MOF is a characteristic we have observed with other cross-linked MOFs and may prove to be a means to modulate guest sorption properties.

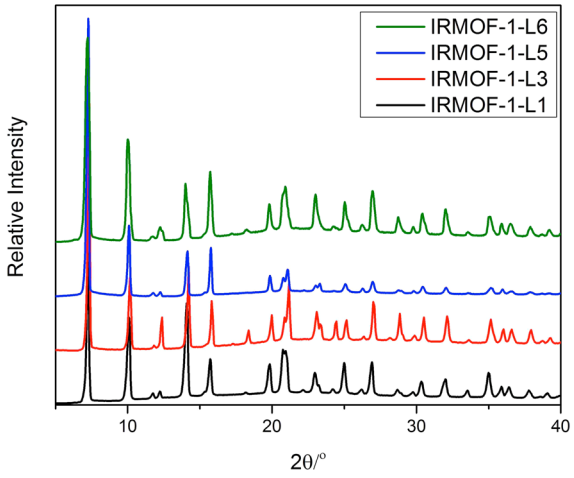

Figure 2. PXRD of IRMOF-1-**L1**, -**L3**, -**L5**, and -**L6** after air-drying from DMF. All of these MOFs show a high degree of uniformity and crystallinity.

In an effort to control the orientation and improve the organization of the cross-linking group, ligands with more rigid tethers were designed and prepared. *Ortho*-, *meta*-, and *para*-xylene dibromides were used to prepare three new ligands (**L2**, **L3**, **L4**) in good yields (Scheme 1, Schemes S1−S2). Of these, the *m*-xylene derivative creates a cross-link that is roughly identical in length to **L1** but with a more rigid structure (Figure 1).[22]

Using standard solvothermal synthetic conditions, only **L3** produced the desired MOF (IRMOF-1-**L3**) as clear truncated blocks (Figure 1). These crystals displayed the expected PXRD pattern for an IRMOF (Figure 2). Despite numerous attempts, under a variety of solvothermal conditions (Table S1), no crystalline materials were obtained using **L2** or **L4**. Under some conditions, **L2** and **L4** produced white powders that were amorphous as gauged by PXRD (data not shown). To obtain the desired ligand orientation (isomer 1, Figure S1), the angle between the linked bdc struts would appear to be too acute with **L2** and too obtuse with **L4**. Only **L3** has the correct geometry to facilitate formation of the IRMOF lattice. Furthermore, **L2** and **L4** are too short to allow for the formation of other cross-linked isomers (Figure S1).

IRMOF-1-**L3** gave a BET surface area of 1619 m^2/g after activation at 105 °C under vacuum. The ^{1}H NMR spectra of digested samples of IRMOF-1-**L3** showed a significant amount of DMF was trapped in the material under these activation conditions (Figure S3). However, the DMF could be removed by heating the material at 150 °C overnight (under a vacuum) giving a BET value of 2121 ± 54 m^2/g (Figure 4). TGA analysis of IRMOF-1-**L3** activated at 105 °C shows a 4% weight loss from 50 to 100 °C but not when activated at 150 °C indicative of complete activation (Figure 3). Activation at either temperature results in a steep 10% weight loss at 350 °C followed by framework degradation at 360 °C (Figure S3). We attribute the 10% weight loss at 350 °C to degradation of the *m*-xylene linker unit. Again, the trapping of solvent in IRMOF-1-**L3** at lower temperatures is suggestive of the potential gating behavior of these materials.

dx.doi.org/10.1021/ic500951b | *Inorg. Chem.* 2014, 53, 7014−7019

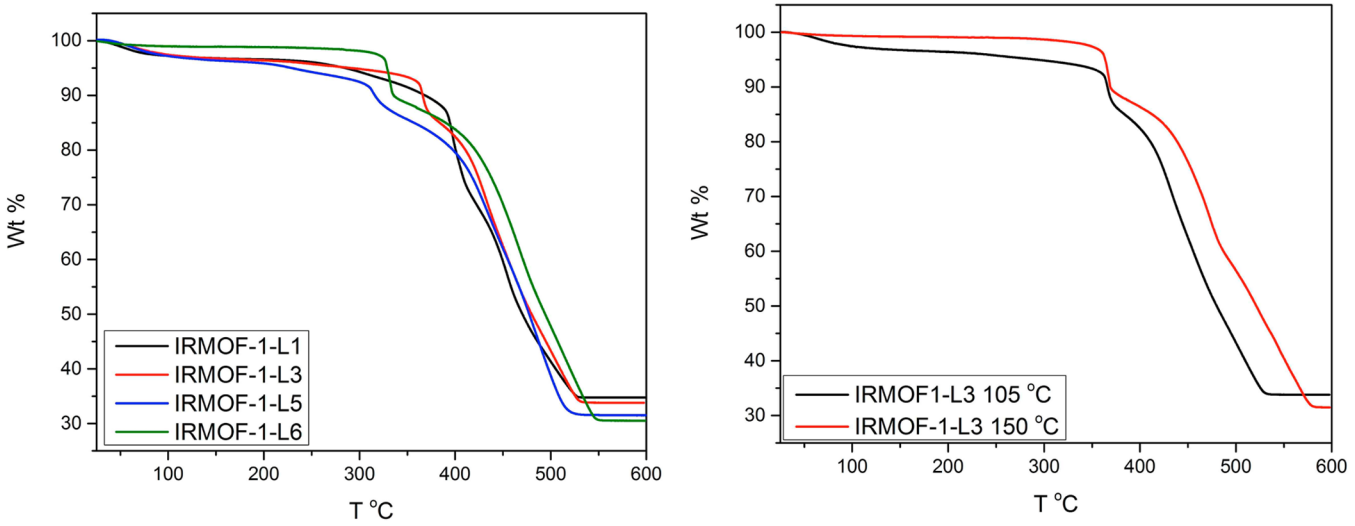

Figure 3. TGA traces of IRMOFs following activation at 105 °C (left). The right graph explicitly shows IRMOF-1-**L3** after both activation at 105 and 150 °C. The distinct weight loss prior to 200 °C at the lower activation temperature is attributed to trapped DMF molecules. A higher activation temperature shows the disappearance of this weight loss, corroborating our assignment.

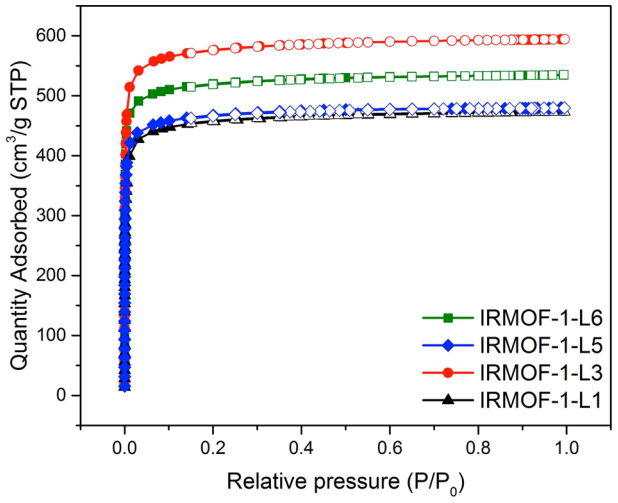

Figure 4. Dinitrogen sorption isotherms of cross-linked IRMOFs (performed at 77 K). Samples were activated at 105 °C (IRMOF-1-**L6**) or 150 °C (all others). The overlap of IRMOF-1-**L1** and **L6** is attributed to the residual solvent trapped in **L1** thus rendering similar sorption properties to the triple bdc linked IRMOF-1-**L6**.

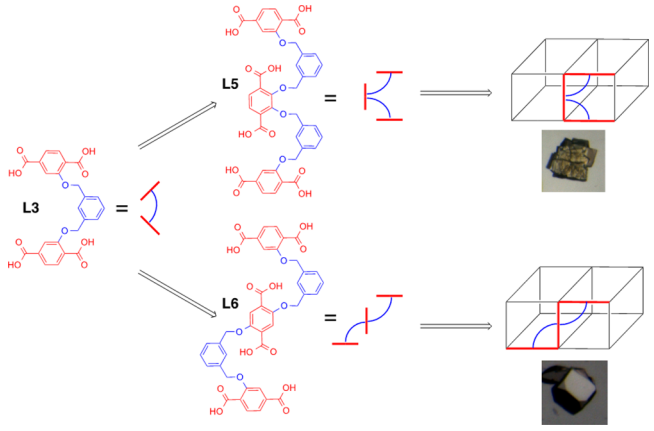

Figure 5. Schematic representation of the design of **L5** and **L6** from **L3**. These oligomeric ligands readily form IRMOF crystals under slow ramping conditions (photographs shown).

XRD structure determination of IRMOF-1-**L3** (Table S2) verified the IRMOF topology but also revealed that parts of the *m*-xylene cross-linker could be located in the difference map. Location of substituents by XRD data is very unusual in the highly symmetric IRMOF system[23,24] and demonstrates that the rigid cross-link is confined to a specific geometry inside the MOF pores. There is some disorder of the cross-linker, but electron density was located for the linker in the expected isomer 1 conformation (Figures S1 and S4), confirming our computational and design analysis. This suggests that by designing ligands that restrict the orientation of the bdc subunits, an increased level of organization and structural predictability can be engineered into the MOF topology.

Successful incorporation of **L3** into the IRMOF structure led to the expansion and evolution of **L3** into ligands **L5** and **L6**. These "oligomeric" type ligands connect three bdc monomers via two *m*-xylene cross-linker units (Figure 5). **L5** and **L6** are 2,3- and 2,5-substitutional isomers of one another, but both limit the bdc units to the isomer 1 orientation (Figure 3, Figure S1). These ligands were synthesized using similar procedures to **L3** as shown in Scheme 1. A Williamson ether synthesis using an excess of 1,3-dibromoxylene provided an intermediate competent for a second coupling in good yields (**6**, Scheme 1). Coupling of the benzyl bromide **6** with one of two diol intermediates, followed by hydrolysis, produced **L5** and **L6** in reasonable yields (Scheme 1).

Our previous cross-linked ligands have required minimal, if any, screening efforts to form IRMOFs. While ligands **L5** and **L6** do form IRMOF under standard solvolthermal conditions, it was found that improved crystal quality and uniformity was achieved by heating with slower temperature ramping (0.5 instead of 2.5 °C/min) and the use of a larger excess of metal ion. The need for slower ramping is consistent with a more demanding "annealing" process that would be required with these oligomeric structures.

Upon combining a 1:12 ratio of **L5** with $Zn(NO_3)_2 \cdot 6H_2O$ in DMF and heating to 100 °C for 24 h, yellow cubes were obtained that were suitable for single-crystal XRD (Figure 5, Table S3). IRMOF-1-**L5** displayed the expected cubic topology,

dx.doi.org/10.1021/ic500951b | *Inorg. Chem.* 2014, 53, 7014−7019

as demonstrated by both the XRD structure and PXRD patterns (Figure 2). Unfortunately, the xylene linker could not be located in the difference map; however, ^{1}H NMR and mass spectral analysis of digested samples confirmed that the ligand remained intact (Figure S5). Activation of the MOF at 105 °C (under vacuum) gave a low BET value of 650 m^2/g and a TGA trace indicative of trapped solvent. By heating at 150 °C (under a vacuum) the BET value was raised to 1654 ± 89 m^2/g (Figure 4). The increased temperature for activation was not surprising as the xylene units occupy a larger percentage of the available pore volume.

To explore how the positioning of the xylyl rings affected the MOF growth and characteristics, **L6** was used in the preparation of a cross-linked IRMOF. Using a 1:10.7 **L6** to zinc ratio, under slow ramping conditions (0.5 °C/min), clear blocks were obtained after 24 h at 100 °C (Figure 5). XRD failed to locate the xylene electron density in the difference map, but again the IRMOF topology was verified by XRD (Table S3) and PXRD (Figure 2). Interestingly, heating at 105 °C was sufficient for complete activation of IRMOF-1-**L6** as corroborated by the high BET value of 1948 ± 34 m^2/g (Figure 4). TGA analysis confirmed no solvent loss at <150 °C followed by MOF degradation at around 380 °C (Figure 3). ^{1}H NMR of the digested material also verified the intact ligand and no residual solvent (Figure S6). Even though the overall number of xylyl groups incorporated is the same as in IRMOF-1-**L5**, the change in orientation of the groups manifests itself in subtly different physical properties of the material.

CONCLUSIONS

In this study, we have synthesized a variety of new cross-linked ligands that eludicate design criteria that are required for the formation of IRMOF under solvothermal conditions. **L1** and **L3** were capable of adhering to the restraints of a cubic lattice because both cross-links, pentane and *m*-xylene, accommodate a specific orientation of the two bdc units. However, **L2** and **L4** that employ *o*- and *p*-xylene linkers were not able to attain the proper geometry, and this was corroborated by an inability to isolate crystalline materials. The characteristics required for successful incorporation of tethered bdc molecules were used to rationally design extended, oligomeric ligands **L5** and **L6**, each possessing six carboxylic acid units per ligand. Amazingly, these also both form IRMOFs. This discovery is a first step toward an advanced level of design and tuning in MOF materials. Expansion of this concept into other frameworks and larger oligomeric and polymeric ligands is currently underway.

ASSOCIATED CONTENT

Supporting Information

Synthetic and experimental details, characterization of compounds, and crystallographic tables. CIF files have been deposited to the Cambridge Structural Database under CCDC 990793-990796. This material is available free of charge via the Internet at http://pubs.acs.org.

AUTHOR INFORMATION

Corresponding Author

*E-mail: scohen@ucsd.edu. Telephone: (858) 822-5596. Fax: (858) 822-5598.

Notes

The authors declare no competing financial interest.

ACKNOWLEDGMENTS

We thank Dr. Min Kim (Chungbuk National University, Korea) for helpful discussions, Dr Y. Su (U.C.S.D.) for performing mass spectrometry experiments, and Dr. C. Moore, Prof. A. Rheingold (U.C.S.D.), and Phuong V. Dau for assistance with single-crystal XRD. This work was supported by a grant from Department of Energy, Office of Basic Energy Sciences, Division of Materials Sciences and Engineering under Award No. DE-FG02-08ER46519. C.A.A. was supported by a National Science Foundation Graduate Research Fellowship under Award No. DGE1144086.

REFERENCES

(1) Rowsell, J. L. C.; Yaghi, O. M. *Microporous Mesoporous Mater.* **2004**, *73*, 3−14.
(2) Tian, D.; Chen, Q.; Li, Y.; Zhang, Y.-H.; Chang, Z.; Bu, X.-H. *Angew. Chem., Int. Ed.* **2013**, *53*, 837−841.
(3) Roy, X.; Hui, J. K. H.; Rabnawaz, M.; Liu, G.; MacLachlan, M. J. *Angew. Chem., Int. Ed.* **2011**, *50*, 1597−1602.
(4) Hurd, J. A.; Vaidhyanathan, R.; Thangadurai, V.; Ratcliffe, C. I.; Moudrakovski, I. L.; Shimizu, G. K. H. *Nat. Chem.* **2009**, *1*, 705−710.
(5) Chen, Z.; Wang, G.; Xu, Z.; Li, H.; Dhôtel, A.; Zeng, X. C.; Chen, B.; Saiter, J.-M.; Tan, L. *Adv. Mater.* **2013**, *25*, 6106−6111.
(6) Li, D.-S.; Zhao, J.; Wu, Y.-P.; Liu, B.; Bai, L.; Zou, K.; Du, M. *Inorg. Chem.* **2013**, *52*, 8091−8098.
(7) Mu, Y.-Q.; Zhu, B.-F.; Li, D.-S.; Guo, D.; Zhao, J.; Ma, L.-F. *Inorg. Chem. Commun.* **2013**, *33*, 86−89.
(8) Medishetty, R.; Tandiana, R.; Koh, L. L.; Vittal, J. J. *Chem.—Eur. J.* **2014**, *20*, 1231−1236.
(9) Distefano, G.; Suzuki, H.; Tsujimoto, M.; Isoda, S.; Bracco, S.; Comotti, A.; Sozzani, P.; Uemura, T.; Kitagawa, S. *Nat. Chem.* **2013**, *5*, 335−341.
(10) Holten-Andersen, N.; Harrington, M. J.; Birkedal, H.; Lee, B. P.; Messersmith, P. B.; Lee, K. Y. C.; Waite, J. H. *Proc. Natl. Acad. Sci. U. S. A.* **2011**, *108*, 2651−2655.
(11) Ma, L.; Wu, C.-D.; Wanderley, M. M.; Lin, W. *Angew. Chem., Int. Ed.* **2010**, *49*, 8244−8248.
(12) Cohen, S. M. *Chem. Rev.* **2012**, *112*, 970−1000.
(13) Ishiwata, T.; Furukawa, Y.; Sugikawa, K. *J. Am. Chem. Soc.* **2013**, *135*, 5427−5432.
(14) Schubert, U. *Chem. Soc. Rev.* **2011**, *40*, 575−582.
(15) Furukawa, Y.; Ishiwata, T.; Sugikawa, K.; Kokado, K.; Sada, K. *Angew. Chem., Int. Ed.* **2012**, *51*, 10566−10569.
(16) Appel, E. A.; Del Barrio, J.; Loh, X. J.; Scherman, O. A. *Chem. Soc. Rev.* **2012**, *41*, 6195−6214.
(17) Allen, C. A.; Boissonnault, J. A.; Cirera, J.; Gulland, R.; Paesani, F.; Cohen, S. M. *Chem. Commun.* **2013**, *49*, 3200−3202.
(18) Tanabe, K. K.; Allen, C. A.; Cohen, S. M. *Angew. Chem., Int. Ed.* **2010**, *49*, 9730−9733.
(19) Huh, S.; Jin, J.; Achard, M. F.; Hardouin, F. *Liq. Cryst.* **1998**, *25*, 285−293.
(20) Eddaoudi, M.; Kim, J.; Rosi, N.; Vodak, D.; Wachter, J.; O'Keeffe, M.; Yaghi, O. M. *Science* **2002**, *295*, 469−472.
(21) Garibay, S. J.; Wang, Z. Q.; Tanabe, K. K.; Cohen, S. M. *Inorg. Chem.* **2009**, *48*, 7341−7349.
(22) Perry; Kravtsov, V. C.; McManus, G. J.; Zaworotko, M. J. *J. Am. Chem. Soc.* **2007**, *129*, 10076−10077.
(23) Dau, P. V.; Polanco, L. R.; Cohen, S. M. *Dalton Trans.* **2013**, *42*, 4013−4018.
(24) Burrows, A. D.; Frost, C. G.; Mahon, M. F.; Richardson, C. *Angew. Chem., Int. Ed.* **2008**, *47*, 8482−8486.